

UNCLASSIFIED

Defense Technical Information Center  
Compilation Part Notice

ADP011139

TITLE: Investigation on a Semi-Active Hydro Mount Using Mr Fluid#

DISTRIBUTION: Approved for public release, distribution unlimited

This paper is part of the following report:

TITLE: Active Control Technology for Enhanced Performance Operational Capabilities of Military Aircraft, Land Vehicles and Sea Vehicles  
[Technologies des systemes a commandes actives pour l'amelioration des performances operationnelles des aeronefs militaires, des vehicules terrestres et des vehicules maritimes]

To order the complete compilation report, use: ADA395700

The component part is provided here to allow users access to individually authored sections of proceedings, annals, symposia, etc. However, the component should be considered within the context of the overall compilation report and not as a stand-alone technical report.

The following component part numbers comprise the compilation report:

ADP011101 thru ADP011178

UNCLASSIFIED

# Investigation on a Semi-Active Hydro Mount Using Mr Fluid<sup>#</sup>

R. Ay<sup>1</sup>, M. F. Golnaraghi<sup>2</sup>, A. Khajepour<sup>3</sup>

1. Exchange Student, Fachbereich Maschinenbau, TU Braunschweig, Schleinitzstr. 8, 38106 Braunschweig, Germany

2. Corresponding Author, Professor, Department of Mechanical Engineering, University of Waterloo, Canada

3. Assistant Professor, Department of Mechanical Engineering, University of Waterloo, Canada

## Abstract

Hydraulic engine mounts (hydro mounts) are passive devices used to isolate automobile engine vibration from the chassis at different automobile operating conditions. In this paper we introduce a semi-active hydro mount, using Magneto Rheologic (MR) fluids. A semi-active hydro mount can be used to optimize the mount performance for a wider range of vehicle operating conditions. The MR fluid mount developed and mathematically modeled in this work can change its yield shear stress once under a magnetic field, and hence, it may be tuned by applying electromagnetic field. The tuning ability allows us to vary the natural frequency of the mount and to increase the damping of the mount. To verify the numerical results an experimental test bed has been developed. Preliminary results show that the experimental and numerical results correlate well.

*Keywords:* Hydraulic engine mounts; Semi-active hydro mounts, Magneto Rheologic (MR) fluid

## 1. Introduction

With the clear thrust of the US Partnership for the New Generation Vehicle (PNGV) effort being mass reduction, the resulting vehicles will suffer from increased vibration levels due to higher engine to frame weight ratios, increased engine force density, and the use of lighter and more flexible vehicle frames. These increased vibration levels will reduce driver comfort and component longevity; the PNGV Sweet 16 does not address this aspect. The engine to frame weight ratio and the engine force densities is increasing in the quest to come-up with lighter and efficient automobiles. Furthermore, lighter and more flexible vehicle frames have led to the increased frame vibration levels. Consequently, recent research and development efforts have been focused on further improvement of engine mounting technology to achieve better vibration isolation, smooth vehicle ride and noise reduction.

Passive hydro-mechanical mounts have been designed to meet the requirements of such a system. A typical hydro mount is designed to have high stiffness and damped response for low frequency large amplitude vibrations (in most cars this is greater than 0.3 mm at 1-50 Hz). Conversely at high frequency small amplitude vibrations, a hydro mount is designed for low stiffness and damping characteristics (amplitudes less than 0.3 mm at 50-300 Hz).

These mounts allow passive adjustment by a variety of hydraulic design options (decoupler, inertia track, rubber shape and stiffness) based on the application and its optimal dynamic properties, engine performance requirements or operating conditions. All these design options allow tailoring the mount characteristics for the specific automotive application. The basic

idea of the hydro mount is to add damping only at the resonant frequency and leave the damping almost unchanged at other frequencies [1-3].

Since a hydro mount can only be tuned for a specific frequency for an optimal performance, it is still a compromise. To further improve the performance of an engine mount to meet the requirements and overcome the limitations, an actively controlled system is required.

The need of an active system has long been recognized and different approaches have been taken to accomplish this [4,5,8]. Similar to the application of Electro-rheological (ER) fluids one can use magneto rheological (MR) fluids to achieve a controllable hydro mount.

In this work we have proposed a semi-active mount system based on MR fluids: non-colloidal suspensions of micron-sized, magnetisable particles in a fluid medium. These fluids have the ability to change from a free-flowing liquid to a semisolid in milliseconds when exposed to a magnetic field, and instantly back to a liquid when the field is removed. They provide simple, quiet, rapid-response, miniaturized, and continuously variable interfaces for electro-mechanical systems. By controlling the applied magnetic field, the fluid's yield stress can be precisely determined, enabling the design of active isolators with minimum weight and maximum control force to eliminate road- and engine-induced vibration.

The objective of this paper is to provide the basic ideas behind an active hydro mount using MR fluid and to design a tunable mount using experimental analysis. The experimental data are used to evaluate the effectiveness of MR fluids on semi-active mounts. This work is intended to provide a basis for future work

<sup>#</sup> Presented and appeared in the Proceedings of NATO, Symposium on Active Control Technology for Enhanced Performance Operational Capabilities of Military Aircraft, Land Vehicles and Sea Vehicles, Braunschweig, Germany, 8-11 May, 2000.

in semi-active mounts using MR fluids. The experimental data can also be used to arrive at an empirical mathematical model.

## 2. Theoretical considerations

### 2.1 Hydro mounts

The ideas of conventional rubber mounts [1] are used in hydro mounts. As in the rubber mounts, the liquid filled mount or hydro mount, offers the possibility of vibration isolation in three orthogonal directions. However, in the primary direction (up down) the mount is very non-linear with frequency due to the fluid resistance and the decoupler action (Figure 1). The non-linearity arrives from the fact that the communicating orifice, connecting two liquid filled chambers, acts as a hydraulic damper, which influences the system due to its resistance to the motion of the fluid. In addition, the decoupler plate has very complicated characteristics, including impact of decoupler plate with the surrounding cage, possibility of turbulent flow, and flow leakage once the decoupler plate has bottomed out [3].

The cross section of a passive, liquid filled hydro mount with inertia track, decoupler, and bell in the upper chamber is shown in Figure 1. The primary rubber element has two functions. It has to carry the static and dynamic load on the mount and it has to act as a piston to pump the liquid through the orifice into the bottom chamber. The ability of the secondary rubber element to bulge will compensate the fluid increase in the lower chamber. Since the secondary rubber compliance acts as an accumulator for liquid passing back and forth through the orifice, it can take the form of a highly flexible diaphragm. When pumping the liquid through the orifice, the primary rubber element will also bulge slightly such that not all the liquid displaced by the piston action is forced through the orifice. The bulging effect of the top and bottom rubber elements is expressed as the change in the chamber volume,  $\Delta V$ , over the pressure change,  $\Delta p$ , also referred to as the compliance of the top and bottom chambers. The unit of the compliance is  $[\text{mm}^3/\text{Pa}] = [\text{mm}^5/\text{N}]$ .

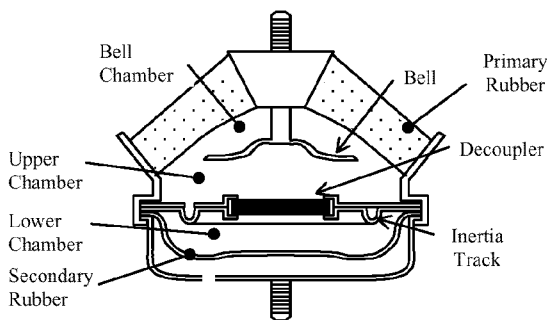


Figure 1. A Model of a Hydro mount

Different approaches have been taken to model a hydro mount [1-3]. Reference [2] describes a linear dynamic model with lumped mechanical and fluid elements. Another study with a non-linear model is by Golnaraghi and Nakhaie [3]. Such models are put up to achieve a dynamic stiffness spectra prediction. The desired characteristic of the hydro mount is the so-called cross point dynamic stiffness, defined as:

$$K^* = \frac{F_T}{x} \quad (1)$$

where  $F_T$  is the transmitted force to the base (chassis) and  $x$  is the excitation amplitude (engine). A typical frequency response curve and also the phase shift curve of a hydro mount with and without implementing a bell are shown in Figure 2 [9].

There are a few design options, which allow for passive tailoring of the mount characteristics for each specific application. These options include variation in the geometry and physical properties of the inertia track, the decoupler, and the mount rubber housing. A detailed description of the above-mentioned options is included in [9].

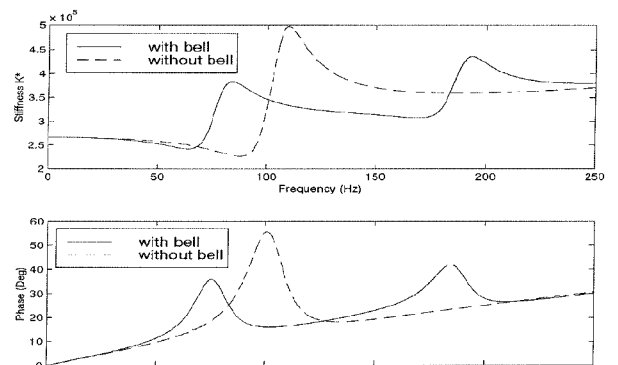


Figure 2. Dynamic Stiffness Curves

In this paper we introduce an idea to be able to actively shift the resonance peaks of the dynamic stiffness curve by external tuning of the mount. In addition to the basic components of a hydro mount MR fluid will be introduced to the system as the active component.

### 2.2 MR fluids

Magneto rheological fluids have been initially discovered by Jacop Rabinow in the 1940's. MR fluids belong to the controllable fluids and are the true magnetic analogues of electro rheological (ER) fluids. They are of interest because of their ability to provide simple, quiet, rapid-response (below 30 msec), miniaturised, and continuously variable interfaces between electronic controls and

mechanical systems. MR fluids are composed of non-colloidal suspensions of micron-sized, magnetisable iron or steel particles in a fluid medium. Water, oil, or silicon based MR fluids are available depending upon the application. In a MR fluid mount, the control action is due to the change in rheological behaviour to an applied external magnetic field. The key to these fluids is their ability to change from a free-flowing liquid to a semisolid in milliseconds when exposed to a magnetic field, and instantly back to a liquid when the field is removed. By applying an external magnetic field the fluid develops a precisely controllable yield stress. A yield stress versus magnetic induction curve for a commercial used fluid (MRF-240BS) is shown in Figure 3.

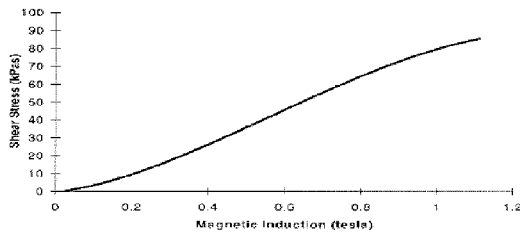


Figure 3. Magnetic Induction Curve (MRF-240BS) [7]

The formation of particle chains (microstructure) when applying a magnetic field restricts the movement of the fluid and thereby increases the viscosity of the suspension. The behaviour of such a controllable fluid is often represented as a Bingham plastic having variable yield strength [6].

MR fluids routinely exhibit dynamic yield strengths of 50–100 kPa for applied magnetic fields of 150 – 250 kA / m (for magnetic induction of 1.3–2.0 Tesla, for commercial used MR fluids). The strength of the fluid is limited by magnetic saturation (see Figure 3). The fluids can be used in a broad temperature range from about -40°C to 150°C and the yield strength varies only slightly over this range. MR fluid exhibits low thermal conductivity (between 0.20–3.80 W / m /°C) and have low coefficients of thermal expansion (between  $0.2 \times 10^{-3}$  and  $0.7 \times 10^{-3}$  in the temperature range from 0 to 150 °C). Temperature range, thermal conductivity, and thermal expansion generally depend upon the carrier fluid [7]. MR fluids have a high resistance to settling. At common flow conditions no separation between the particles and carrier fluid is observed.

Concentration and density of particles, particle size and shape distribution, properties of the carrier fluid, additional additives, applied field, and temperature are what the rheological properties of controllable fluids depend on. The interdependency of these factors is very complex and has not yet been completely discovered. Therefore, it is important to optimise the performance of the MR fluids for particular applications.

One of the three basic modes of operation is the fixed pole or pressure driven flow mode. The fixed pole mode is also referred to as the valve mode. Figure 4 illustrates how the valves can be accomplished with no moving parts.

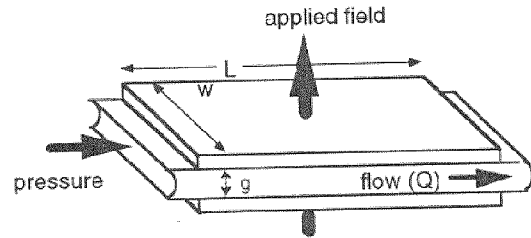


Figure 4. Fixed Pole Operating Mode [6]

The pressure drop developed across the device shown in Figure 4 is divided into a:

$$\text{Viscous component:} \quad \Delta P_{\eta} = \frac{12 \eta Q L}{g^3 w} \quad (2)$$

$$\text{Field dependent component:} \quad \Delta P_{\tau} = \frac{c \tau_y L}{g} \quad (3)$$

where  $\eta$  is the plastic viscosity,  $Q$  the volumetric flow rate,  $L$  the length,  $g$  the gap,  $w$  the width,  $\tau_y$  the yield stress developed in response to an applied external magnetic field  $H$ , and  $c$  is a parameter which ranges from a minimum value of 2 (for  $\Delta P_{\tau} / \Delta P_{\eta}$  less than 1) to a maximum value of 3 (for  $\Delta P_{\tau} / \Delta P_{\eta}$  greater than 100) [6].

The total pressure drop in the device is approximately equal to the sum of  $\Delta P_{\tau}$  and  $\Delta P_{\eta}$ . When algebraically manipulate Eq. (2) and Eq. (3) a different derived design equation can be provided

$$V = \frac{12}{c^2} \left( \frac{\eta}{\tau_y^2} \right) \left( \frac{\Delta P_{\tau}}{\Delta P_{\eta}} \right) Q \Delta P_{\tau} \quad (4)$$

where  $\eta/\tau_y^2$  are fluid material properties,  $\Delta P_{\tau} / \Delta P_{\eta}$  is the control ratio (or dynamic range), and  $Q \Delta P_{\tau}$  is the mechanical power level,  $V$  is the minimum active fluid volume ( $V = Lwg$ ). The minimum active fluid volume  $V$  is the volume which is necessary in order to achieve the desired control ratio at a given flow rate with a specified controlled pressure drop  $\Delta P_{\tau}$ .

The dynamic range  $\lambda = \Delta P_{\tau} / \Delta P_{\eta}$  involves the viscous properties of the MR fluid (i.e.,  $\eta$  and  $\tau_y$ ). In reality, the dynamic range of a device may also be significantly a function of other device properties such as seal and bearing friction.

### 3. Performance criteria

The fluid resistance due to the orifice and valve element influences the overall damping of the system (magnitude of the peak in the dynamic stiffness curve). Eq. (3) states that a change in pressure drop results in a change in shear stress of the fluid. The pressure drop across the valve is related to the fluid resistance (pressure drop-flow relation) as:

$$(P_1 - P_2)_{total} = R_f Q \quad (5)$$

where  $Q$  is the volumetric flow and  $R_f$  is the fluid flow resistance which is influenced by changing the shear stress. The emphasis of the experiments is to find whether the variable shear stress of the fluid within the valve element is also able to shift the resonance peaks.

As discussed earlier, the MR fluid behaves like a Bingham fluid, in which, before reaching the yield shear stress, the core flows like a solid (similar to toothpaste flow). The size of the solid core is increased or decreased according to the magnitude of shear stress. An increase in the size of solid core will increase the cross sectional area of the flowing fluid and also the mass of moving fluid. Since the area is proportional to the mass, the inertia of the fluid within the valve element will decrease as according to

$$I = \frac{\rho \cdot l}{A} = \frac{m}{A^2} \quad (6)$$

where  $\rho$  is the density of the fluid,  $l$  is the length of the valve,  $A$  is the cross-sectional area, and  $m$  is the mass of fluid in the valve. The controllable shear stress could be thought of as a controllable orifice size. Changing the orifice size will result in changing the system inertia, Eq. (6), or system natural frequency. Shifting the natural frequency was observed before in [3] using same concept.

When applying a magnetic field to the fluid in the valve element, the pressure in the upper chamber has to exceed a threshold pressure set by the yield shear stress of the fluid in order to allow for the fluid to pass through the mount valve into the lower chamber. This threshold pressure is set by the strength of the magnetic field. Unless the threshold pressure is reached, the valve would block the flow. In this case, the overall stiffness of the system would mainly be determined by the upper chamber compliance, the lower chamber compliance would not have any effect. Notice that in this case the mount will act similar to a regular rubber mount.

### 4. Designing the mount model

In this section the design of a proposed model of a semi-active hydro mount using MR fluid is discussed. For the mount model it

is desirable to have the possibility to easily change the overall stiffness. The general approach is to design a model that has the flexibility to be used in different tests for various modifications of the hydro mount. These modifications are different number of chambers, different compliances, and different orifices. This flexibility is achieved through a modular design. The fundamental concepts of a lumped parameter fluid system model are used as a base for the design process. Since the emphasis of research is the dynamic effects of an active valve, the well-known linear Voigt model representing the primary rubber element (stiffness and damping) is not included in the design. This could later be implemented in a mathematical model to see the actual performance of the semi-active hydro mount. The model consists of an actuator, two chambers connected through a valve element, two devices representing the primary and secondary rubber element compliance, a magnetic circuit to activate the valve, and the incompressible MR fluid.

To model the pumping action of the primary rubber element a hydraulic cylinder is used as an ordinary piston pump. The piston pump accomplishes two main functions. Besides the pumping action, it also represents the upper chamber volume. The bore size of the cylinder is selected to be 3.81 cm (1.5 inches).

The importance of the compliance elements arises from the fact that the overall stiffness of the system mainly depends upon them. To model the compliance, two basic ideas are investigated, the use of spring-loaded piston pumps or the use of accumulators. The advantage of using spring-loaded piston pumps is the flexibility of achieving different compliance values by using different springs or pistons. The compliance can be evaluated as

$$C = \frac{A^2}{k} \quad (7)$$

where  $A$  is the cross sectional area of the piston and  $k$  is the stiffness of the spring. Another advantage of this configuration is having a constant stiffness over the full operation of the piston. The disadvantages of this configuration are the seals of the piston and the piston rod. The seals experience Coulomb friction and would therefore negatively effect the dynamics of the overall system.

To avoid the negative effects, commercially available diaphragm accumulators have been selected for the actual model of the semi-active hydro mount. The accumulators work in the following manner. They have a reservoir, which is filled with a compressible gas such as nitrogen or air. If the pressure in the system outside the reservoir exceeds the pressure of the gas, the gas will be compressed; the pressure change will be compensated to a certain degree. The enclosed gas in the reservoir has a stiffness value depending on the volume and the pressure. Since the stiffness can be converted into a compliance value, an accumulator can be used to model a compliance element. To

determine the compliance of the accumulators, the simplified model shown in Figure 5 is used.

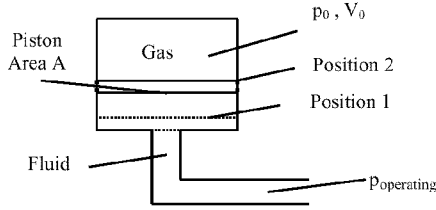


Figure 5. Simplified Model of an Accumulator

Position 1 is referred to as the pre-charged position and Position 2 represents the operating point. A few assumptions are made before stating the relationship for the compliance. The change of states of the ideal gas is assumed to be isothermal and the pressure in the accumulator and the one in the system is assumed to be in equilibrium.

The isothermal change of the states can be represented as follows:

$$p_1 \cdot V_1 = p_2 \cdot V_2 = \text{const.} \quad (8)$$

Therefore,

$$p \cdot V = (p + \Delta p) \cdot (V - \Delta V) \quad (9)$$

$$p \cdot V = p \cdot V + \Delta p \cdot V - p \cdot \Delta V - \Delta p \cdot \Delta V \quad (10)$$

The term  $\Delta p \Delta V$  was neglected since only small changes are considered. Eq. (10) is arranged to

$$p \cdot \Delta V = \Delta p \cdot V \quad (11)$$

Knowing that

$$\Delta V = A \cdot \Delta x \quad (12)$$

where  $\Delta x$  is the displacement of the diaphragm and  $A$  is the cross sectional area which remains the same. For the steady state the stiffness of the gas can be represented as spring stiffness. The spring tension can be stated as:

$$\Delta F = k \cdot \Delta x \quad (13)$$

where the spring tension is in equilibrium with the force due to the pressure

$$\Delta F = \Delta p \cdot A \quad (14)$$

Substituting Eq. (12)-(14) into Eq. (11) gives a statement for the stiffness of the accumulator.

$$k = \frac{A^2 \cdot p}{V} \quad (15)$$

where  $p$  is the pre-charged pressure of the accumulator and  $V$  is the nominal volume of the gas in the reservoir. Using Eq. (7) gives an expression for the compliance:

$$C = \frac{V_0}{p_0} \quad (16)$$

where  $V_0$  and  $p_0$  are the volume and the pressure of the accumulator at the operating point, respectively. The stiffness of the gas is not constant, and therefore, a non-linear relationship between compliance and pressure is expected. When exciting the system at different operating pressures, different compliance values will be seen. Nevertheless, the compliance values of the accumulators are assumed to be constant once the pressure of the system is brought to the operating point. Only small pressure changes are expected when exciting the system.

Two different accumulators are used in this work. One has a 75ml reservoir handling operating pressures up to 250 bar and the other one has a 160ml reservoir handling the same pressure.

The size of the valve element determines the active fluid volume specified in (4). The volumetric flow rate and therefore, the required controllable mechanical power level are not known, and have to be found experimentally. Therefore, the equation for the minimum active fluid volume cannot be used for designing purposes in this particular case. The valve is designed to add as less inertia to the system as possible. Therefore the valve has a large cross sectional area and a short length (6). The Ampere-turns, generating the magnetic field, strongly depends upon the size of the valve, since the valve with the fluid inside will be part of the magnetic circuit. The valve has to be shaped in such a way that the magnetic core of the magnetic circuit can easily be interfaced. Quadratic shaped pole pieces are chosen with which a quadratic cross-section of 17 x 5 mm of the valve element is formed. Material considerations are very important since the flow channel is directly part of the magnetic circuit. If high permeable carbon sheet steel is used, the magnetic flux lines will go directly through the material without affecting the fluid (Figure 6b). For this reason very low permeable stainless steel sheet is used. In the magnetic circuit the core material, the stainless steel sheet of the valve element, and the fluid are in series as shown in Figure 6a.

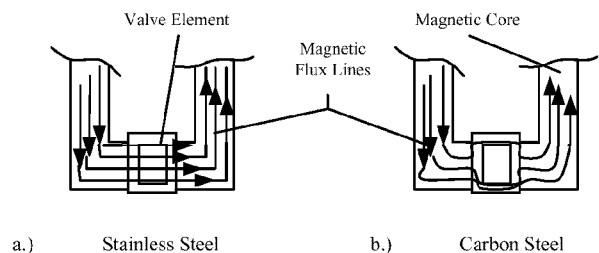


Figure 6. The Magnetic Circuit Including the Valve Element

In the last mentioned configuration, using stainless steel, which has a low permeability value of 1.3, the thickness of the sheet will almost act as an air gap and therefore high Ampere-turns are needed in order to achieve the required magnetic field within the fluid.

A more effective design was considered in this work. Figure 7 shows the cross section of the valve. As shown, carbon sheet metal was used at the long sides, which will be in direct contact with the magnetic core material, and stainless steel sheet metal was used on the short sides. Therefore, there will be no air gap effect and also no magnetic flux short. The magnetic flux can now be assumed to go straight through the fluid, of course with some leakage on the edges. Both sheet materials are 1.2 mm thick and were welded along their edges to form the quadratic shaped cross section. The length of the valve part was chosen to be 10 mm.

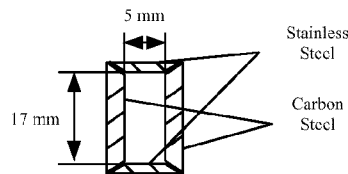


Figure 7. Valve Element-Cross-Section

Two main considerations can be pointed out when choosing the MR fluid. Firstly, the fluid had to be chemically compatible with all the other parts of the system, including seal materials as well as the diaphragm material of the accumulators. Secondly, the right carrier fluid had to be chosen accounting for lubrication aspects. The MRF-132LD fluid with a density of  $3040 \text{ kg/m}^3$  was chosen because of its good dynamic viscosity and density values. The fluid can build up yield shear stresses up to 54 kPa at magnetic flux densities of 1.2 Tesla.

The magnetic circuit represents the variable interface between electronic control and mechanical system and provides the required magnetic field to the fluid needed to change its state. The field must be applied perpendicular to the direction of fluid flow. The parts of the magnetic circuit are: the iron core, the coil, which supplies the magnetomotive force, the valve element, and the MR fluid. The magnetic circuit was capable to achieve the required magnetic field strength around the fluid. The circuit was designed in such way that the required field strength was reached at 2.6 A and 14.6 V. A variable power supply was used to tune the valve as needed.

A schematic of the overall model can be seen in Figure 8. A not so large reservoir was considered as the lower chamber of the system. The connector between valve, accumulator, and the pressure transducer was representing it. The system holds approximately 80 ml of the MR fluid. Since no feedback systems

implemented into the system yet, the first model of the hydro mount using MR fluid is really considered to be an external tunable mount. A semi-active control unit is later on implemented, to actively tune the mount in response to the vibrations it is exposed to.

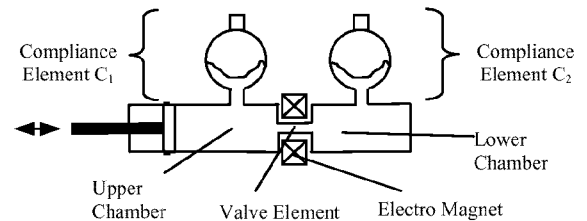


Figure 8. Overall Model of the Mount

## 5. Description of Experiments

A hydraulic operating dynamic testing machine was used in the experiments. Due to the frequency limitations of the test machine, the excitation amplitude dropped rapidly at higher frequencies. Hence, we could not test the mount performance in a more realistic frequency range of 200 to 250 Hz. However, the tests within the frequency range of 0 to 20 Hz, show great merit. Excitation amplitudes up to  $\pm 0.44 \text{ mm}$  were achievable for the frequencies up to 20 Hz.

To monitor and select the pressures during the experiments, two pressure transducers were used. The pressure was measured in each chamber, on both sides of the valve element, in addition to the displacement of the actuator. The signal from the displacement sensor and the signal from the two pressure transducers were fed into a data conditioner card. The signal was low pass filtered at 70 Hz and then amplified in order to get an appropriate resolution when reading the data into the data acquisition card. The amplified and filtered data were fed into a 486 PC processing.

Tests were conducted initially to verify the mount model, and to confirm if it were designed properly to perform as intended, like a hydro mount. In addition experimental data were collected to achieve insight into the feasibility of this system for use as a semi-active mount in the future. Hence, the first experiments were made to form the basis of future experiments.

In the initial studies, different pre-charge pressures for the accumulators were tried out as well as different operating pressure points, which are directly dependent upon the zero point of the excitation piston. It could be seen that when pre-charging the accumulators to very low levels, it was hard to distinguish the peak to peak values of the pressures, since the accumulators were more capable to compensate for the pumped fluid. According to the tests made, it is recommended to keep the pre-charge pressure

in either of the accumulators above 0.8 bar (11.5 psi). The main experiments can be subdivided into three parts.

### 5.1 Fluid performance

Several tests were conducted to check the performance of the MR fluid. The accumulators were pre-charged to no particular values ( $P_{01}=19\text{psi}$ ,  $P_{02}=45\text{psi}$ ), and the system was excited with a harmonic input with a frequency of 10 Hz and displacement amplitude of 1.7 mm (peak to peak). The system was working around an operating pressure of approximately 48 psi. The current going through the coil, producing the magneto-motive force was stepped through 0 to 2.61 A, and different shear stresses of the fluid were observed. A typical data set printout is shown in Figure 9. In this case, the pressure P2 (lower chamber pressure) response has reached steady state above a current of around 1 A. It could be further recognized that the peak to peak value of the pressure P1 (upper chamber pressure) also did not change anymore in the same region of current.

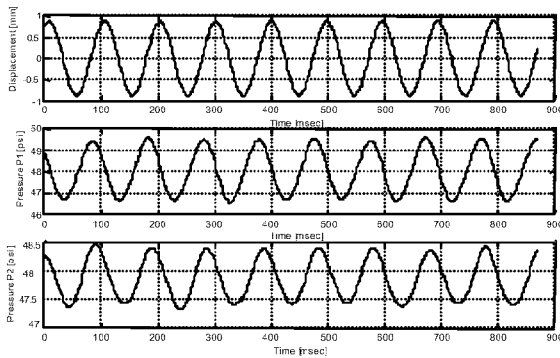


Figure 9. Typical Time Response Curves (0 A,  $C_1=19\text{psi}$ ,  $C_2=45\text{psi}$ )

### 5.2 Frequency sweep

In this part of the tests, the excitation frequency was varied through 0 to 20 Hz in 11 equally distributed steps. These tests were performed to see how the system behaves at a frequency sweep. There was no magnetic field applied to the valve part. The accumulators were set to 20 psi and 45 psi for  $P_{01}$  and  $P_{02}$ , respectively. The system was then brought to an operating pressure of approximately 48 psi. The excitation amplitude was kept the same throughout the frequency sweep. The value was the pre-determined maximum amplitude for 20 Hz, 0.88 mm. The test was then repeated. But before the next tests were performed, a rough magnitude calculation was done to predict the natural frequency of the system. The natural frequency was estimated as [1]

$$\omega_N = 2 \cdot \pi \cdot f_N = \sqrt{\frac{1}{I_i} \cdot \left( \frac{1}{C_1} + \frac{1}{C_2} \right)} \quad (17)$$

where  $I_i$  is the inertia of the valve element and  $C_1$  and  $C_2$  are the compliance values. The pre-charged pressure of the accumulators ( $P_{01}$  and  $P_{02}$ ) as well as the net volume of them, 75 ml and 160 ml, were used to determine the volume of the air within the accumulators ( $V_{OP1}$  and  $V_{OP2}$ ) at the operating pressure point (8). The found volume and the operating pressure ( $P_{OP}$ ) were plugged into (16) to achieve the compliance of the accumulators at operating pressure. The inertia of the valve is determined with (6). The compliance values and the inertia of the valve element could then be used to estimate the natural frequency of the system (17). Several iterations have been performed to get the natural frequency of the system within the 20 Hz. Another three tests have been performed. The values can be seen in Table 1.

Table 1. Values to Determine Resonance Frequency

|                             |           |                        |                        |                        |
|-----------------------------|-----------|------------------------|------------------------|------------------------|
| $P_{01}$ [psi]              | 20        | 37                     | 20                     | 12                     |
| $P_{02}$ [psi]              | 45        | 35                     | 19                     | 9                      |
| $P_{OP}$ [psi]              | 48        | 41                     | 24                     | 13                     |
| $V_{OP1}$ [m <sup>3</sup> ] |           | $6.768 \times 10^{-5}$ | $6.25 \times 10^{-5}$  | $6.923 \times 10^{-5}$ |
| $V_{OP2}$ [m <sup>3</sup> ] |           | $1.366 \times 10^{-4}$ | $1.267 \times 10^{-4}$ | $1.108 \times 10^{-4}$ |
| $C_1$ [m <sup>5</sup> /N]   |           | $2.39 \times 10^{-10}$ | $3.77 \times 10^{-10}$ | $7.72 \times 10^{-10}$ |
| $C_2$ [m <sup>5</sup> /N]   |           | $4.83 \times 10^{-10}$ | $7.65 \times 10^{-10}$ | $1.23 \times 10^{-9}$  |
| $I_i$ [kg/m <sup>4</sup> ]  | 357647.06 | 357647.06              | 357647.06              | 357647.06              |
| $f_N$ [Hz]                  | 29.8      | 21.04                  | 16.74                  | 12.21                  |

### 5.3 Resonance frequency shift

The last part, which required the most number of tests, was intended to find out whether changing the magnetic field strength could shift the frequency response curves. In this part of the experiments, the accumulators were both pre-charged to 34 psi and the operating point was brought up to 41 psi. This almost matches the settings of a previous test, which was giving the most reasonable results. For various frequencies in between 0 and 20 Hz, data was collected for different applied magnetic fields. Therefore, the current was stepped through 0 to 0.5 A. The frequency was kept constant and the data was collected for each current step before switching to the next frequency. That could be done, since the MR fluid does not show considerable hysteresis loops. The values for the compliance of the upper and lower chamber were  $2.264 \times 10^{-10} \text{ m}^5/\text{N}$  and  $4.692 \times 10^{-10} \text{ m}^5/\text{N}$ , respectively.

## 6. Results and discussion

The following data was extracted from the time response curves to perform the evaluation of the results:

- the mean value of the piston road position
- the average of the maximum displacement of the piston road
- the frequency of the input signal
- the average of the peak to peak values of pressure P1
- the mean value for the pressure P1

- the average of the peak to peak values of pressure P2
- the mean value of pressure P2

In the presented graphs in this section, the peak to peak values of the pressures P1 and P2 have been used to plot over the frequency or the current. Usually the maximum pressures are used for evaluation purposes of hydro mounts. Since it could not be ensured that the piston rod of the exciting machine moves exactly around the same point for each data collection, the peak to peak values have been used. The position of excitation varies only slightly. But already small variation in position would make it hard to evaluate the data. The input was a sinusoidal displacement, and therefore the peak to peak value of the pressure indicates the same behavior as the maximum values. Consider the excitation around a fixed point, when the maximum pressure increases, the peak to peak value increases as well, the increase would be twice as high as the increase of the maximum value.

### 6.1 Fluid performance

The results of two tests are shown in Figures 10a and b. The current was stepped through 0 to 1.2 A for the first one and through 0 to 0.5 A for the second one. All the other tests of this section indicated the same behavior and gave the same results. Delta P1 represents the pressure change in the upper chamber and delta P2 in the lower chamber. The pre-charge pressures and the operating pressure are shown in Table 1.

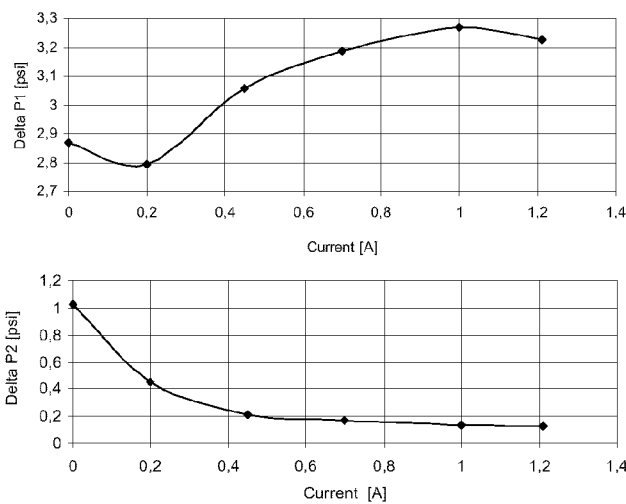


Figure 10a. Delta P vs. Current (0 – 1.2 A)

The exact frequency for these tests was found to be 10.42 Hz. Figure 10a clearly indicates that the pressure difference (delta P1) increases as the current increases. It can also be seen that the curve plateaus after a certain increase in current. The leveling was even better indicated for the test stepping up to 2.6 A with the current.

That clearly indicates that the pressure built up in the upper chamber was not sufficient enough any more to work against the shear stress of the fluid and therefore can not pump the fluid through the orifice. As a reminder, the maximum achievable yield shear stress of the fluid

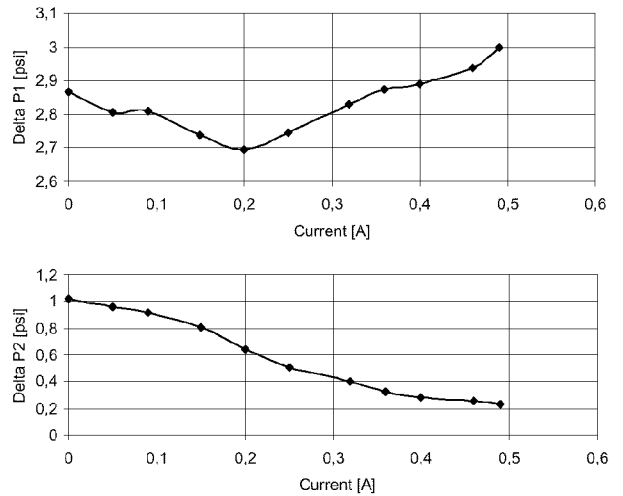


Figure 10b. Delta P vs. Current (0 – 0.5 A)

is theoretically reached around 2.6 A, but the leveling starts already way before that point. That confirms the just stated prediction. It can be assumed the valve is blocked. The applied current range of 0 to 0.5 A (Figure 10b) was not sufficient high enough to see the leveling. At both delta P1 curves a minimum could be observed around 0.2 A, which may not be explained yet at this stage.

The contrary change of delta P2 compared to the upper chamber can be recognized in both plots. That makes sense, since less fluid is pumped through the valve element, and therefore the pressure built up in the lower chamber will be less. The delta P2 curves seem to plateau before delta P1. This fact could not be explained yet, at this state of the experiments. Furthermore, the decrease in delta P2 was slightly higher than the increase of delta P1. This results in the different compliance values of the two chambers; the value of C2 was twenty times as large as the value of C1. Nothing could be seen in contrast to the minimum of the delta P1 curve around 0.2 Ampere.

To be complete, the pre-charge pressures of 19 psi, for the upper chamber representing compliance element, and 45 psi, for the lower chamber representing compliance element as well as the operating pressure of 48 psi results in compliance values of  $8.97 \times 10^{-11} \text{ m}^5/\text{N}$  for the upper and  $4.53 \times 10^{-10} \text{ m}^5/\text{N}$  for the lower compliance element.

### 6.2 Frequency sweep

In Figure 11 the results of the tests with the theoretical calculated resonance frequency at 21.04 Hz and 12.21 Hz are presented. The delta-P vs. Frequency curves indicate a non-linear relationship between those variables. It can be seen that the delta P1 values as well as the delta P2 values of both cases are heading towards a maximum point, which will occur at resonance frequency (natural frequency of the system). Even knowing that the theoretically determined resonance frequency of the second case (Figure 11b) suppose to be at 12.21 Hz, no peak in the curves could be observed for delta P1 neither for P2. However, it can be seen that the slope of the curves, for the second case, at higher frequencies decreased in comparison to the previous case (Figure 11a) and also that the maximum value of delta P1 and P2 at approximately 24 Hz increased slightly. This indicates that the maximum was shifted towards lower frequencies and therefore the natural frequency was shifted. It could also be observed for both delta P2 curves that there was a slight minimum between 5 and 10 Hz which then delays the increase of delta P2 in comparison to delta P1. This phenomena still needs to be explained.

Nevertheless, the typical behavior of a hydro mount with a simple orifice, since no magnetic field was applied, could be shown with this part of the tests. In the first set of experiments, it was not possible to get the natural frequency within the frequency range of 0 to 22 Hz. That indicates that the assumptions made to estimate the natural frequency of the system have to be thought over and then be implemented into an estimation formula for the natural frequency again. The assumptions include things such as neglecting the effects of the diaphragms of the accumulators.

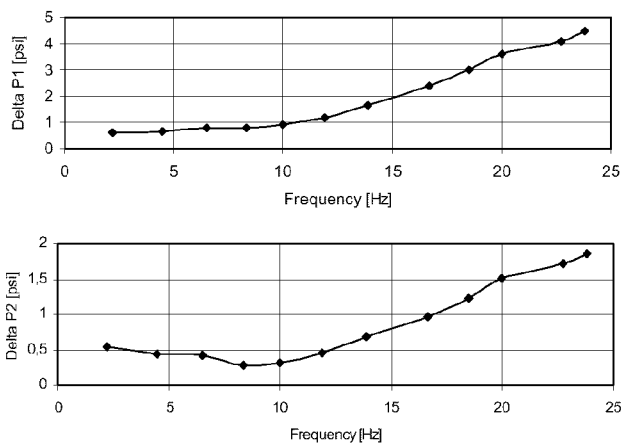


Figure 11a. Delta P vs. Frequency ( $P_{01}=37$  psi,  $P_{02}=35$  psi)

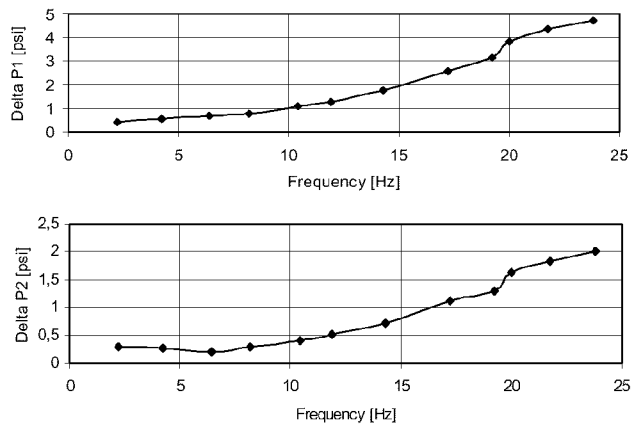


Figure 11b. Delta P vs. Frequency ( $P_{01}=12$  psi,  $P_{02}=9$  psi)

### 6.3 Resonance frequency shift

The peak to peak values of the pressure P1 and pressure P2 vs. Frequency curves are shown in Figure 12 for different currents producing the magnetic field. With this test the results of the previous tests could be confirmed, especially when looking at the curves for zero Ampere. The delta P2 increases with a slight delay and the minimum between 5 and 10 Hz could be seen again.

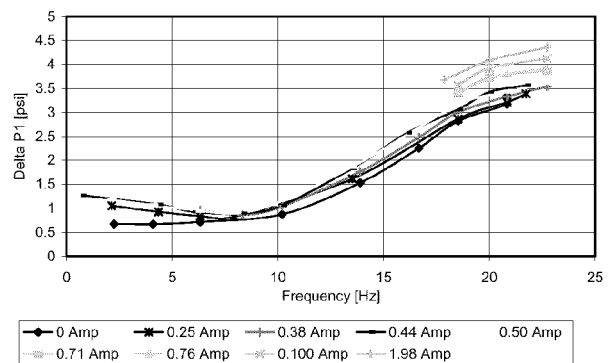


Figure 12a. Delta P1 vs. Frequency for different Currents

When looking at the delta P1 vs. frequency curve in Figure 12a, one basically recognizes that the curves are shifted towards higher values. Taking a closer look, one sees that the curves forming a minimum below 10 Hz. The minimum is getting more distinguishable as the current goes up. The minimum seems to be formed around 8 Hz. A shift of the curve, and hence, a shift of the resonance frequency, is hard to see since the resonance frequency was not reached within the 22 Hz. But one could assume a shift of the resonance peak, since the distance between the graphs change along the frequency, particularly for curves representing current

values of 0.71 A and higher. It was realized to late during the test, that the current could have been increase even further before seeing the blocking effect of the valve. Therefore only fractions of the curves from 0.71 to 1.98 A are shown.

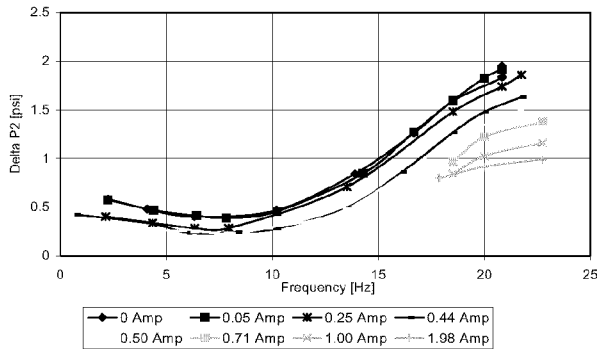


Figure 12b. Delta P2 vs. Frequency for different Currents

It can also be recognised that the delta P2 vs. Frequency curves are shifted to lower values when increasing the current. Taking a look at Figure 12b would lead to the conclusion that the minimum, recognised below 10 Hz, is straightened out when applying higher currents. That would be in contrary with the forming of a minimum for the delta P1 curves. Again it can be assumed that the resonance peak was shifted to a different frequency, since the distances between the curves changes with increase of the current, therefore the slope of the curves at a particular frequency is different.

## 7. Conclusion

A model of an external tunable hydro mount using the magneto rheological fluid MRF-132LD was designed, constructed, and tested. The important components of the system included a valve, magnetic circuit, and MR fluid, which represent the active components, and excitation piston and compliance elements. The results of the experimental investigations in general confirm the right choice of shapes and sizes. The typical behavior of a hydro mount was observed in preliminary tests.

Experiments have been performed within the limited frequency range of 0 to 22 Hz. Due to the test setup limitations, the accumulators were adjusted in such a way that the natural frequency of the system was brought close to the maximum achievable 22 Hz with the required displacement. The values of the pressures in both chambers predicted a heading towards a resonance peak with increasing frequencies. In further tests it was shown that the damping of the system could be adjusted by varying the applied magnetic field. This was indicated by an increasing or decreasing pressure in the upper chamber, caused by the changing of the yield shear stress of the fluid within the valve part. The pressure data obtained from the tests suggested a shift of

the pressure peak, in both chambers, when changing the applied magnetic field. This suggests the proposed system may be used as an active system.

In future studies, feedback will be added to study the performance of the system as an active mount.

## Acknowledgements

The authors acknowledge and thank the Lord Corporation for providing a supply of MR Fluid and for its technical support. The authors would also like to thank the technical staff: Marius van Reenen, Ernst Huber, and Clarence Wallace for their assistance and advice in the manufacturing of the testing equipment. This project was supported in part by Natural Sciences and Engineering Council of Canada.

## References

- [1] R. Singh, G. Kim, P. V. Ravindra, "Linear Analysis of Automotive Hydro-Mechanical Mount with Emphasis on Decoupler Characteristics", Department of Mechanical Engineering, The Ohio State University, Columbus, June 1991, *Journal of Sound and Vibration* (1992) 158(2), 219-243.
- [2] W. C. Flower, "Understanding Hydro Mounts for Improved Vehicle Noise, Vibration and Ride Qualities", Lord Corporation, Erie, PA, 1985.
- [3] M. F. Golnaraghi and G.R. Nakhaie, "Development and Analysis of a Simplified Nonlinear Model of a Hydraulic Engine Mount", Presented in the 8th Conference on Nonlinear Vibrations, Stability and Dynamics of Structures, July 23-27, 2000 VPI/SU, Virginia. Also Submitted for publication in the *Journal of Vibration and Control*.
- [4] T. G. Duclos, "An Externally Hydraulic Mount which uses Electro-Rheological Fluid", SAE Paper #870963.
- [5] A. Genesseeux, "Research for New Vibration Isolation Techniques: From Hydro-Mounts to Active Mounts", SAE Paper #931324, 1993.
- [6] J. D. Carlson, D. M. Catanzarite, K. A. St. Clair, "Commercial Magneto-Rheological Fluid Devices", Lord Corporation, July (1995), LL-8001.
- [7] M. R. Jolly, J. W. Bender, J. D. Carlson, "Properties and Applications of Commercial Magnetorheological Fluids", Lord Corporation, March (1998).
- [8] P. L. Graf, F. Shourehi, "Modelling and Implementation of Semi-Active Hydraulic Engine Mounts", ASME, Vol. 110, 422-429, Dec. 1988.
- [9] A. A. Geissberger, A. Khajepour and M.F. Golnaraghi, "Nonlinear Modelling and Experimental Verification of a MDOF Hydraulic Engine Mount", To appear in the ASME, AMD Proceeding, symposium on Active noise and vibration control, November 5-10, 2000.